Applying Metallo-Organic Ligand Design Principles to the Stereoselective Synthesis of a Peptide-Based $Pd_2L_4X_4$ Cage

Dominic F. Brightwell[‡,b] Kushal Samanta[‡,c] Jimmy Muldoon,[a] Patricia C. Fleming,[a] Yannick Ortin,[a] Lina Mardiana,[d,e,f] Paul G. Waddell,[d] Michael J. Hall,[d] Ewan R. Clark,[g] Felipe Fantuzzi,[b] Aniello Palma*[a]

[a] *School of Chemistry, University College Dublin, Belfield, Dublin 4, Ireland.*

[b] *Supramolecular and Interfacial Chemistry Group, School of Chemistry and Forensic Science, Park Wood Rd, Ingram building, The University of Kent, Canterbury CT2 7NZ, Kent, United Kingdom.*

[c] *School of Chemistry, University of Birmingham, Edgbaston, Birmingham, B15 2TT, UK.*

[d] *Chemistry – School of Natural and Environmental Sciences, Bedson Building, Newcastle University, Newcastle upon Tyne, Tyne and Wear NE1 7RU, UK.*

[e] *Indicatrix Crystallography Ltd, Bedson Building, Newcastle University, Newcastle upon Tyne, Tyne and Wear NE1 7RU, UK.*

[f] *Department of Chemistry, Universitas Indonesia, Depok, Jawa Barat, Indonesia.*

[g] *School of Science, The University of Greenwich, Chatham Maritime, Chatham, Kent, UK.*

[‡]*These authors contributed equally to this work.*

Corresponding author: aniello.palma@ucd.ie

TOC:

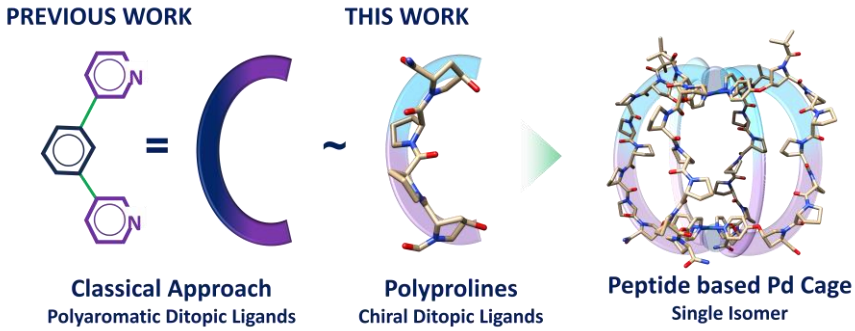

ABSTRACT: *The rational and controlled synthesis of metallo-organic cages using polyaromatic ligands is well established in the literature. There is a strong interest to advance this field towards the use of chiral ligands capable of yielding cages in a stereoselective manner. Herein, we demonstrate that the classical approach for designing metallo-organic cages can be translated to polyproline peptides, a biocompatible class of chiral ligands. We have successfully designed a series of polyprolines, which mimic the topology of ditopic polyaromatic ligands, to yield the stereoselective synthesis of a novel Pd lantern cage. This work will pave the way towards the stereospecific synthesis of more complex, functionalized peptide cages.*

Inspired by nature's unparalleled control over self-assembly processes, chemists have long been pursuing the synthesis of supramolecular constructs in a controlled and predictable manner. [1,2] Metallo-organic cages are a class of discrete supramolecular non-covalent constructs for which a large set of assembly rules have been successfully established.[1–3] The seminal work of Stang, Raymond, Fujita, and Nitschke identified a number of design principles which allow the geometry of metallo-organic constructs to be predicted (e.g. cages or MOFs, M vs L ratio, geometry of the cage).[4–8] Furthermore, software developed to assist synthetic chemists to rationally design these constructs and predict their properties has recently been introduced in the literature.[9,10] However, in scoping the literature associated with these non-covalent hosts, it is evident that the large majority of ligands used are highly symmetric and are typically of a polyaromatic nature.[8,11–13] This approach is commonly used as it simplifies the assembly process (Figure 1).

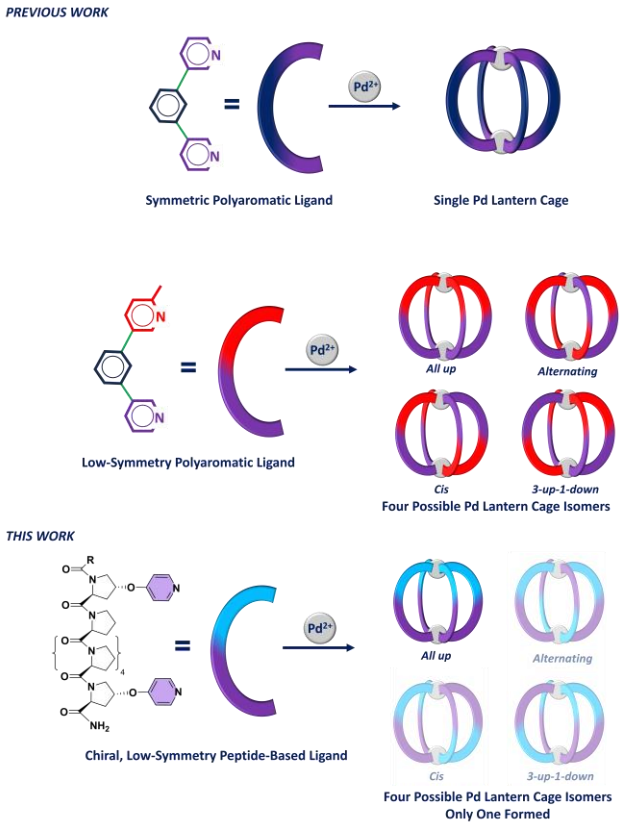

Figure 1. Schematic representation of symmetric polyaromatic ligands and low-symmetry ligands (previous work). Schematic representation of the polyproline peptide used in this work to yield a Pd lantern cage stereoselectively (this work).

While some encouraging reports are appearing,[12,14,15] challenges still remain when attempting to synthesize asymmetric constructs. With the aim of developing systems closer to those found in nature, moving away from polyaromatic structures, Fujita reported the use of simple oligopeptides with pyridine units at the N and C termini. These peptides form either coordination networks or a series of complex and entangled metallo-peptide rings when exposed to metals ions (typically Ag^{+}).[16,17] Clever also recently reported the use of a functionalized cyclic peptide as a ligand for the synthesis of a Pd^{2+} peptide complex.[18] These reports have been instrumental in redirecting this field towards the use of biocompatible ligands. However, these impressive peptide-based nano-constructs are typically serendipitously discovered, rendering their manipulation and functionalization extremely challenging. It is evident that the design principles developed for polyaromatic ligands cannot be applied to the types of peptide-based ligands currently being reported in the literature. Building upon our previous work,[19,20] herein, we successfully

demonstrate that using polyproline helices as supramolecular peptide building blocks, it is possible to translate the design principles developed for classical polyaromatic ligands to peptide-based ligands. Moreover, the peptide-based cage reported herein is able to stabilize a reactive species generated *in situ*. These findings represent a pivotal discovery towards the future design of highly functionalized cavities capable of mimicking natural enzymes. The classical ligands used in the assembly of metallo-cages are typically rigid (i.e., polyaromatic) and they can be treated as rod-like structures that retain their directionality throughout the self-assembly process.[8,21,22] Moreover, the bite angles,[21] the relative position of the two coordinating groups on the ligand backbone, are well defined. Therefore, structural rigidity and positional control of the coordinating groups are clearly key parameters which should be conserved in the ideal peptide-based ligand.

Polyproline helices are secondary structures which appear in most proteins. In contrast to other helices used in supramolecular chemistry, the polyproline helix is retained even in exceptionally short and un-functionalized sequences (e.g., four prolines).[19,20,23] We have recently demonstrated that it is possible to predict, with high accuracy, the spatial position of functional groups introduced onto the backbone of polyproline helices (Figure 2a).[20]

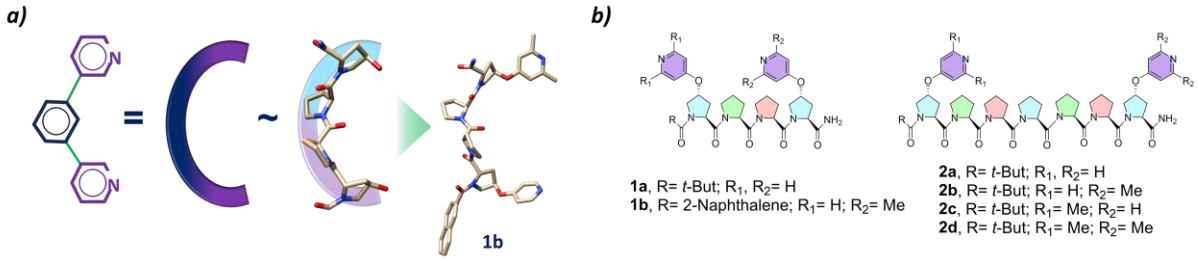

Figure 2. a) SC-XRD of **1b** used to demonstrate how its spatial arrangement mimics the classical C shape of ditopic ligands. b) Polyprolines used in this work. Proline rings color-coded according to their helical face.

Our recent work also demonstrates the resilience of these helices to functional groups, which is unparalleled when compared to other peptide-based secondary structures.[24] Therefore, the polyproline helix periodicity (*i*+3), the persistent rod-like shape, and the ability to functionalize the peptide backbone with a high level of positional control, inspired us to use these peptides as ditopic ligands in the rational synthesis of peptide-based cages. While this manuscript was in preparation, a similar peptide system was

used to yield palladium cages.[25] Interestingly, their system has been shown to favour the formation of a different type of cage isomer from the one reported herein, demonstrating the complementarity of our work. These investigations were conducted simultaneously and independently by the two groups. The first class of ligand we choose to mimic with the polyproline helix was the di-pyridine ditopic ligand typically employed with Pd^{2+} salts to synthesize lantern shaped metallo-cages.[7] We have recently demonstrated via SC-XRD, that the hydroxyl groups of *trans*-hydroxyproline (Hyp) in the peptide AcHyp-Pro-Pro-HypNH_2 are facing away from the peptide backbone and on the same polyproline face (Figure 2a).[20] This spatial arrangement mimics the classical C shape of ditopic ligands used in the synthesis of lantern shaped Pd^{2+} cages. We hypothesized that further functionalization with a coordinating group would result in a peptide-based ligand which should follow the same predictable behavior as the classical polyaromatic ditopic ligands. The introduction of the coordinating group on position 4 of the proline was achieved starting from protected *cis*-hydroxyproline (ESI). Polyprolines **1a-b** and **2a-d** were synthesized using solid-phase-peptide-synthesis (SPPS) and purified by preparative HPLC (Figure 2b, ESI). To our delight, we were able to crystallize compound **1b** from slow evaporation of a saturated methanol solution (ESI). In line with our previous works, the SC-XRD analysis of the structure confirmed that both the predicted absolute stereochemistry (Flack parameter = 0.07(14)) and the polyproline II secondary structure had been retained for **1b** (Figure 2a).[19,20] Peptide **1a** was capped with a pivalic amide at the N-terminus to remove any rotamers in solution, hence simplifying the interpretation of the NMR data.[26] A solution of **1a** in D_2O was treated with 0.5 eq of $Pd(ACN)_4(BF_4)_2$ and heated at 338 K for 2 h. ^{1}H-NMR and ^{1}H-DOSY analysis showed full conversion of **1a** into a mixture of two species (Figure 3; D[m^2/s] = 1.89 e^{-10} and 1.96 e^{-10}).

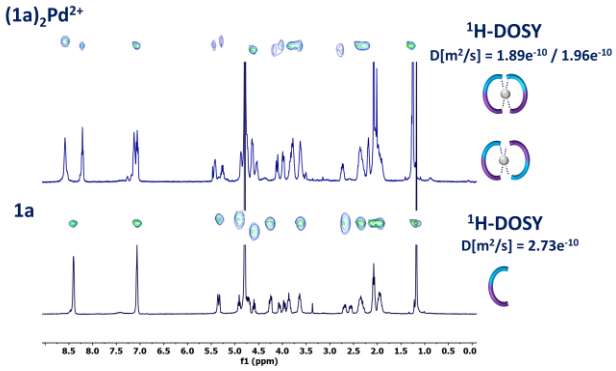

Figure 3. Stacking of ^{1}H-NMR and ^{1}H-DOSY for **1a** and **$(1a)_2Pd^{2+}$**.

LC-HRMS showed that the species present in solution were doubly charged (ESI). The chromatogram trace showed two peaks each with the same mass, charge, and isotopic patterns. These results suggest that the polyproline tetramer **1a** behaves like a chelating ligand forming a ML_2^{2+} complex, rather than the desired $M_2L_4^{4+}$ cage. We concluded that the two species in solution were the two isomers of $\mathbf{(1a)_2Pd^{2+}}$ (Figure 3). As polyproline helices show a periodicity of *i*+3, the heptameric peptide **2a** was synthesized with the intention of preparing an elongated ligand with the same topology as **1a-b**. We hypothesized that the spacing between the two pyridine groups in **2a** would promote the formation of the desired $\mathbf{(2a)_4Pd_2^{4+}}$ cage. A solution of **2a** was treated with 0.5 eq of $Pd(ACN)_4(BF_4)_2$ and heated at 338K for 2h. ^{1}H-NMR analysis showed conversion of **2a** into a single new species and HRMS confirmed this species to be the desired tetra charged lantern cage. 1D, 2D and ^{1}H-DOSY NMR analysis confirmed the presence of a single species in solution (Figure 4). Circular dichroism (CD) studies, showed that **2a** and $\mathbf{(2a)_4Pd_2^{4+}}$ retained the polyproline II conformation (ESI)

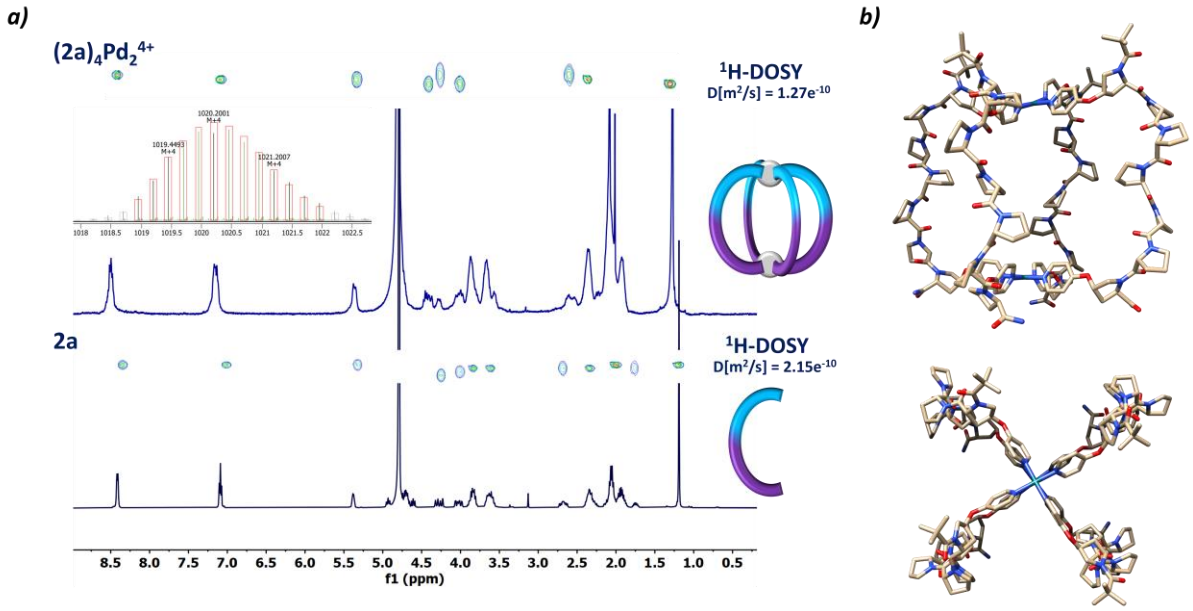

Figure 4. a) Stacking of ^{1}H-NMR and ^{1}H-DOSY for **2a** and $\mathbf{(2a)_4Pd_2^{4+}}$; HRMS insert of the tetra charged complex. b) Side view and top view of $\mathbf{(2a)_4Pd_2^{4+}}$ model (ESI for details), hydrogens are removed for clarity.

In the case of asymmetric ligands such as **2a**, there are four possible $Pd_2L_4^{4+}$ isomers that can form in solution (see figure 1); remarkably, $\mathbf{(2a)_4Pd_2^{4+}}$ is formed in a stereoselective manner. Of the four possible

cage isomers, due to their symmetry, only two of them can yield a ^{1}H-NMR spectrum which is consistent with the one obtained for $\mathbf{(2a)_4Pd_2^{4+}}$, the *all-up* or the *alternating* isomer. The *3-up-1-down* isomer can be excluded as this would yield a highly complex ^{1}H-NMR, as each peptide pillar would be in a different chemical environment. The *cis* isomer can also be excluded as its symmetry would yield a ^{1}H-NMR spectrum with double the number of signals compared to **2a** (e.g. the tert-butyl would show as two singlets, each integrating for eighteen protons). As both sets of aromatic peaks for the pyridines at the N and C terminals overlap in the complex and in **2a** (Figure 4), NOESY NMR could not be used to interrogate the geometry of this isomer (ESI). Moreover, attempts to crystallize this cage were unsuccessful. To probe the geometry of $\mathbf{(2a)_4Pd_2^{4+}}$ around the metal centres, we decided to modulate the steric bulk of the pyridyl groups. We hypothesised that if the peptides in $\mathbf{(2a)_4Pd_2^{4+}}$ are in the *all up* conformation, the assembly of peptides **2b-c** into cages would not be successful as the steric demand around the Pd centre coordinating the four lutidines would be too high. On the other hand, if it is the alternating isomer which is forming in solution, treatment of **2b-c** with Pd^{2+} salt should yield a lantern cage as the major product, as the steric demand would be much lower in this case, with two lutidines coordinating to each metal centre. In support of our hypothesis, peptide **2d** successfully demonstrated that the lantern geometry could not be achieved with four lutidines around the metal centre, as no complex formation occurred when **2d** was treated with 0.5eq of $Pd(ACN)_4(BF_4)_2$ (see NMR analysis in ESI). When **2b** and **2c** are treated separately with Pd^{2+} salt, complicated mixtures of products were observed in the ^{1}H-NMR with some precipitate forming in both cases (ESI). These results suggest that cage $\mathbf{(2a)_4Pd_2^{4+}}$ adopts the *all-up* geometry. To explore this further, a detailed computational investigation of the four possible isomers was performed based on distinct computational approaches. Given the large size of the systems, each containing nearly 550 atoms, full density functional theory (DFT) calculations for obtaining optimized geometries were impractical. Therefore, we performed geometry optimizations using four distinct approaches (ESI). Of these approaches, the optimization of the cages through classical molecular mechanics (MM) with the universal force field (UFF)[28] coupled with SAMSON's automatic molecular structure perception was successful and smoothly led to reasonable cage structures.[29] Single-point calculations at the PBE0[30,31]-D3[32](BJ)[33]/def2-SVP[34]+SMD[35](water) level of theory on the optimized cages, after DFT re-optimization of the hydrogens, revealed a slight preference for the *all-up* geometry over the other three isomers, with the *all-up* geometry being more stable than the *alternating* structure by 1.93 kJ

mol⁻¹. These computational results support our experimental findings. The stability of the **(2a)$_4$Pd$_2^{4+}$** was monitored via NMR studies. ^{1}H- and ^{19}F-NMR spectra were recorded for the same sample stored at room temperature in an NMR tube over a period of four months (Figure 5a). While no changes were visible in the ^{1}H-NMR, after a few months a new peak emerged in the ^{19}F-NMR spectrum. The chemical shift of this peak (-131.47 ppm, internal reference TFA) and the presence of satellite peaks consistent with a ^{29}Si-^{19}F coupling (108 Hz), indicate that this species is $[SiF_6]^{2-}$.[36]

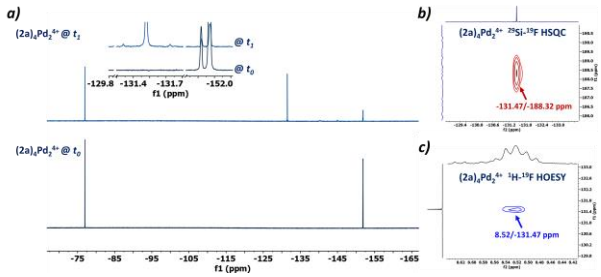

Figure 5. a) Stacking of ^{19}F-NMR spectra at t_0 (recorded as soon as synthesized) and t_1 recorded after four months. b) ^{29}Si-^{19}F HSQC and c) ^{1}H-^{19}F HOESY spectra of **(2a)$_4$Pd$_2^{4+}$** demonstrating through space engagement between the cage and $[SiF_6]^{2-}$.

A ^{29}Si-^{19}F HSQC experiment confirmed the presence of a silicon atom (-188.32 ppm) directly bound to the fluorine atoms at -131.47 ppm (Figure 5b); the silicon chemical shift is consistent with literature reports for SiF_6^{2-}. While the formation of SiF_6^{2-} *in situ* due to the slow decomposition of BF_4^- in aqueous environment (pH 7.4) in a silicate glass tube, is not unexpected, the survival of this anion at this pH in unbuffered D_2O is surprising.[37,38] Metallo-organic cages capable of stabilizing a reactive species have been reported in the literature,[39–41] and our data suggests that **(2a)$_4$Pd$_2^{4+}$** behaves in a similar manner. We hypothesize that **(2a)$_4$Pd$_2^{4+}$** is engaging with the reactive anion SiF_6^{2-}, preventing its hydrolysis. ^{1}H-^{19}F HOESY experiments were performed to probe our hypothesis and investigate any supramolecular engagement of the anion with the peptide cage. Through space correlation between the fluorine signal at -131.47 ppm and the aromatic proton of the pyridine at 8.52 ppm of **(2a)$_4$Pd$_2^{4+}$** was established by ^{1}H-^{19}F HOESY experiments (Figure 5c; ESI). These results strongly suggest that **(2a)$_4$Pd$_2^{4+}$** is engaging with the reactive anion formed *in situ*, stabilizing it, and preventing its hydrolysis in neutral aqueous solution.

In conclusion, we have successfully demonstrated the stereoselective and rational synthesis of a polyproline-based Pd-cage. We have demonstrated that the classical approach towards the rational design of organometallic cages can be translated to polyproline helices. Moreover, this peptide cage can engage and stabilize a reactive species formed *in situ*. Future work will explore the ability of these polyproline-based cages to act as catalysts capable of stabilizing reactive intermediates. These findings will pave the way towards the stereospecific synthesis of more complex, functionalized peptide cages for applications in host-guest chemistry, catalysis, and chemical separation. These results will be reported in due course.

References

(1) Raynal, M.; Ballester, P.; Vidal-Ferran, A.; Van Leeuwen, P. W. N. M. Supramolecular Catalysis. Part 2: Artificial Enzyme Mimics. *Chemical Society Reviews*. 2014, pp 1734–1787. https://doi.org/10.1039/c3cs60037h.

(2) Pullen, S.; Tessarolo, J.; Clever, G. H. Increasing Structural and Functional Complexity in Self-Assembled Coordination Cages. *Chemical Science*. **2021**, 12 (*21*), 7269–7293. https://doi.org/10.1039/d1sc01226f.

(3) Brown, C. J.; Toste, F. D.; Bergman, R. G.; Raymond, K. N. Supramolecular Catalysis in Metal–Ligand Cluster Hosts. *Chem. Rev.* **2015**, *115* (9), 3012–3035. https://doi.org/10.1021/cr4001226.

(4) Caulder, D. L.; Raymond, K. N. The Rational Design of High Symmetry Coordination Clusters. *Journal of the Chemical Society - Dalton Transactions*. **1999**, 8, 1185–1200. https://doi.org/10.1039/a808370c.

(5) Sawada, T.; Matsumoto, A.; Fujita, M. Coordination-Driven Folding and Assembly of a Short Peptide into a Protein-like Two-Nanometer-Sized Channel. *Angew. Chemie - Int. Ed.* **2014**, *53* (28), 7228–7232. https://doi.org/10.1002/anie.201403506.

(6) Castilla, A. M.; Ramsay, W. J.; Nitschke, J. R. Stereochemistry in Subcomponent Self-Assembly. *Acc. Chem. Res.* **2014**, *47* (7), 2063–2073. https://doi.org/10.1021/ar5000924.

(7) McTernan, C. T.; Davies, J. A.; Nitschke, J. R. Beyond Platonic: How to Build Metal-Organic Polyhedra Capable of Binding Low-Symmetry, Information-Rich Molecular Cargoes. *Chemical Reviews*. **2022**, 122, (11) 10393–10437. https://doi.org/10.1021/acs.chemrev.1c00763.

(8) Cook, T. R.; Zheng, Y. R.; Stang, P. J. Metal-Organic Frameworks and Self-Assembled Supramolecular Coordination Complexes: Comparing and Contrasting the Design, Synthesis, and Functionality of Metal-Organic Materials. *Chemical Reviews*. **2013**, 113, (1), 734–777. https://doi.org/10.1021/cr3002824.

(9) Jelfs, K. E. Computational Modeling to Assist in the Discovery of Supramolecular Materials. *Ann. N. Y. Acad. Sci.* **2022**, *1518* (1), 106–119. https://doi.org/10.1111/NYAS.14913.

(10) Piskorz, T. K.; Martí-Centelles, V.; Young, T. A.; Lusby, P. J.; Duarte, F. Computational Modeling of Supramolecular Metallo-Organic Cages-Challenges and Opportunities. *ACS Catalysis*. American Chemical Society **2022**, 12, (10), 5806–5826. https://doi.org/10.1021/acscatal.2c00837.

(11) Northrop, B. H.; Zheng, Y. R.; Ki-Whan, C. H. I.; Stang, P. J. Self-Organization in Coordination-Driven Self-Assembly. *Acc. Chem. Res.* **2009**, *42* (10), 1554–1563. https://doi.org/10.1021/ar900077c.

(12) Bloch, W. M.; Clever, G. H. Integrative Self-Sorting of Coordination Cages Based on "naked" Metal Ions. *Chem. Commun.* **2017**, *53* (61), 8506–8516. https://doi.org/10.1039/c7cc03379f.

(13) Jurček, O.; Bonakdarzadeh, P.; Kalenius, E.; Linnanto, J. M.; Groessl, M.; Knochenmuss, R.; Ihalainen, J. A.; Rissanen, K. Superchiral Pd 3 L 6 Coordination Complex and Its Reversible Structural Conversion into Pd 3 L 3 Cl 6 Metallocycles. *Angew. Chemie* **2015**, *127* (51), 15682–15687. https://doi.org/10.1002/ange.201506539.

(14) Wu, K.; Benchimol, E.; Baksi, A.; Clever, G. H. Non-Statistical Assembly of Multicomponent [Pd2ABCD] Cages. *Nat. Chem. 2024 164* **2024**, *16* (4), 584–591. https://doi.org/10.1038/s41557-023-01415-7.

(15) Benchimol, E.; Regeni, I.; Zhang, B.; Kabiri, M.; Holstein, J. J.; Clever, G. H. Heteromeric Completive Self-Sorting in Coordination Cage Systems. *J. Am. Chem. Soc.* **2024**, *146* (10), 6905–6911. https://doi.org/10.1021/JACS.3C14168/SUPPL_FILE/JA3C14168_SI_001.PDF.

(16) Sawada, T.; Fujita, M. Folding and Assembly of Metal-Linked Peptidic Nanostructures. *Chem*. **2020**, 6, 1861–1876. https://doi.org/10.1016/j.chempr.2020.07.002.

(17) Sawada, T.; Saito, A.; Tamiya, K.; Shimokawa, K.; Hisada, Y.; Fujita, M. Metal–Peptide Rings Form Highly Entangled Topologically Inequivalent Frameworks with the Same Ring- and Crossing-

Numbers. *Nat. Commun.* **2019**, *10* (1), 921. https://doi.org/10.1038/s41467-019-08879-7.

(18) Schulte, T. R.; Holstein, J. J.; Schneider, L.; Adam, A.; Haberhauer, G.; Clever, G. H. A New Mechanically-Interlocked [Pd2L4] Cage Motif by Dimerization of Two Peptide-Based Lemniscates. *Angew. Chemie - Int. Ed.* **2020**, *59* (50), 22489–22493. https://doi.org/10.1002/anie.202010995.

(19) Brightwell, D. F.; Truccolo, G.; Samanta, K.; Fenn, E. J.; Holder, S. J.; Shepherd, H. J.; Hawes, C. S.; Palma, A. A Reversibly Porous Supramolecular Peptide Framework. *Chem. - A Eur. J.* **2022**, *28* (66), e202202368. https://doi.org/10.1002/chem.202202368.

(20) Brightwell, D. F.; Truccolo, G.; Samanta, K.; Shepherd, H. J.; Palma, A. Supramolecular Self-Assembly of Engineered Polyproline Helices. *ACS Macro Lett.* **2023**, *12* (7), 908–914. https://doi.org/10.1021/acsmacrolett.3c00304.

(21) Cook, T. R.; Stang, P. J. Recent Developments in the Preparation and Chemistry of Metallacycles and Metallacages via Coordination. *Chem. Rev.* **2015**, *115* (15), 7001–7045. https://doi.org/10.1021/cr5005666.

(22) Caulder, D. L.; Raymond, K. N. Supermolecules by Design. *Accounts of Chemical Research*. American Chemical Society **1999**, 32, (11), 975–982. https://doi.org/10.1021/ar970224v.

(23) Kakinoki, S.; Hirano, Y.; Oka, M. On the Stability of Polyproline-I and II Structures of Proline Oligopeptides. *Polym. Bull.* **2005**, *53* (2), 109–115. https://doi.org/10.1007/s00289-004-0317-6.

(24) Morales, P.; Jiménez, M. A. Design and Structural Characterisation of Monomeric Water-Soluble α-Helix and β-Hairpin Peptides: State-of-the-Art. *Archives of Biochemistry and Biophysics*. **2019**, 32, (11), 149–167. https://doi.org/10.1016/j.abb.2018.11.014.

(25) Barber, B. E.; Jamieson, E. M. G.; White, L. E. M.; Mcternan, C. T. Metal-Peptidic Cages – Helical Oligoprolines Generate Highly Anisotropic Nanospaces with Emergent Isomer Control. **2023**. https://doi.org/10.26434/CHEMRXIV-2023-89MZ0.

(26) Costantini, N. V.; Ganguly, H. K.; Martin, M. I.; Wenzell, N. A.; Yap, G. P. A.; Zondlo, N. J. The Distinct Conformational Landscapes of 4S-Substituted Prolines That Promote an Endo Ring Pucker. *Chem. - A Eur. J.* **2019**, *25* (48), 11356–11364. https://doi.org/10.1002/chem.201902382.

(27) Yoshizawa, M.; Nagao, M.; Kumazawa, K.; Fujita, M. Side Chain-Directed Complementary Cis-Coordination of Two Pyridines on Pd(II): Selective Multicomponent Assembly of Square-, Rectangular-, and Trigonal Prism-Shaped Molecules. *J. Organomet. Chem.* **2005**, *690* (23), 5383–5388. https://doi.org/10.1016/j.jorganchem.2005.06.022.

(28) Bannwarth, C.; Ehlert, S.; Grimme, S. GFN2-XTB—An Accurate and Broadly Parametrized Self-Consistent Tight-Binding Quantum Chemical Method with Multipole Electrostatics and Density-Dependent Dispersion Contributions. *J. Chem. Theory Comput.* **2019**, *15* (3), 1652–1671. https://doi.org/10.1021/acs.jctc.8b01176.

(29) Artemova, S.; Jaillet, L.; Redon, S. Automatic Molecular Structure Perception for the Universal Force Field. *J. Comput. Chem.* **2016**, *37* (13), 1191–1205. https://doi.org/10.1002/jcc.24309.

(30) Adamo, C.; Barone, V. Toward Reliable Density Functional Methods without Adjustable Parameters: The PBE0 Model. *J. Chem. Phys.* **1999**, *110* (13), 6158–6170. https://doi.org/10.1063/1.478522.

(31) Ernzerhof, M.; Scuseria, G. E. Assessment of the Perdew–Burke–Ernzerhof Exchange-Correlation Functional. *J. Chem. Phys.* **1999**, *110* (11), 5029–5036. https://doi.org/10.1063/1.478401.

(32) Grimme, S.; Antony, J.; Ehrlich, S.; Krieg, H. A Consistent and Accurate Ab Initio Parametrization of Density Functional Dispersion Correction (DFT-D) for the 94 Elements H-Pu. *J. Chem. Phys.* **2010**, *132* (15), 154104. https://doi.org/10.1063/1.3382344.

(33) Grimme, S.; Ehrlich, S.; Goerigk, L. Effect of the Damping Function in Dispersion Corrected Density Functional Theory. *J. Comput. Chem.* **2011**, *32* (7), 1456–1465. https://doi.org/10.1002/jcc.21759.

(34) Weigend, F.; Ahlrichs, R. Balanced Basis Sets of Split Valence, Triple Zeta Valence and Quadruple Zeta Valence Quality for H to Rn: Design and Assessment of Accuracy. *Phys. Chem. Chem. Phys.* **2005**, *7* (18), 3297–3305. https://doi.org/10.1039/b508541a.

(35) Marenich, A. V.; Cramer, C. J.; Truhlar, D. G. Universal Solvation Model Based on Solute Electron Density and on a Continuum Model of the Solvent Defined by the Bulk Dielectric Constant and Atomic Surface Tensions. *J. Phys. Chem. B* **2009**, *113* (18), 6378–6396. https://doi.org/10.1021/jp810292n.

(36) Christe, K. O.; Wilson, W. W. Nuclear Magnetic Resonance Spectrum of the Fluoride Anion. *J. Fluor. Chem.* **1990**, *46* (2), 339–342. https://doi.org/10.1016/S0022-1139(00)81000-3.

(37) Urbansky, E. T. Fate of Fluorosilicate Drinking Water Additives. *Chem. Rev.* **2002**, *102* (8), 2837–2854. https://doi.org/10.1021/cr020403c.

(38) Finney, W. F.; Wilson, E.; Callender, A.; Morris, M. D.; Beck, L. W. Reexamination of Hexafluorosilicate Hydrolysis by 19F NMR and PH Measurement. *Environ. Sci. Technol.* **2006**, *40* (8), 2572–2577. https://doi.org/10.1021/es052295s.

(39) Mal, P.; Breiner, B.; Rissanen, K.; Nitschke, J. R. White Phosphorus Is Air-Stable within a Self-Assembled Tetrahedral Capsule. *Science (80-.).* **2009**, *324* (5935), 1697–1699. https://doi.org/10.1126/SCIENCE.1175313.

(40) Rothschild, D. A.; Tran, A.; Lipke, M. C. Mingling Light, Oxygen, and Organometallics to Form Cobalt-Carbon Bonds in the Confines of a Metal-Organic Nanocage. *Organometallics* **2023**, *42* (22), 3219–3226. https://doi.org/10.1021/ACS.ORGANOMET.3C00358/SUPPL_FILE/OM3C00358_SI_001.PDF.

(41) Banerjee, R.; Chakraborty, D.; Mukherjee, P. S. Molecular Barrels as Potential Hosts: From Synthesis to Applications. *Journal of the American Chemical Society*. **2023**, 145, (14), 7692–7711. https://doi.org/10.1021/jacs.3c01084.

Supporting Information:

CCDC 2360407 and 2362367 contain the supplementary crystallographic data for this paper. These data can be obtained free of charge from The Cambridge Crystallographic Data Centre via www.ccdc.cam.ac.uk/structures.

Author Contributions:

DFB and KS contributed equally to this work. AP, DFB, KS, performed the synthesis purification and data analysis for all species synthesized herein. ERC, PCF and YO were involved with the collection of non-routine NMR experiments and together with AP, DFB and KS to their interpretation. FF undertook the computational study. JM performed all LC-HRMS experiments and data processing. MJH, LM and PGW undertook and supported crystallization experiments and single crystal X-ray diffraction analysis for **1b**. The manuscript was written through contributions of all authors. All authors have given approval to the final version of the manuscript.

Acknowledgements:

AP, DFB and KS thank EPSRC (grant EP/T016140/1) for their generous financial support. FF acknowledges the financial and computational support provided by the University of Kent and Julius-Maximilians-Universität Würzburg. Special thanks are extended to Dr. Timothy Kinnear for his invaluable assistance with high-performance computing. JM thank the Comprehensive Molecular Analysis Platform (CMAP) initiative under the SFI Research Infrastructure Programme in 2019 (grant 18/RI/5702) for the generous support of the LCMS facilities. PCF, YO thank SFI (grant 12/RI/2341) and UCD Equip Funding Programme – 2020 and 2022 for the generous support of the NMR facilities. MJH, LM and PGW thank the Engineering and Physical Sciences Research Council (grant EP/W021129/1) for single crystal X-ray diffraction facilities.

Conflict of Interests:

The authors declare no conflict of interest.